

Nanoscale

Accepted Manuscript



This is an *Accepted Manuscript*, which has been through the Royal Society of Chemistry peer review process and has been accepted for publication.

Accepted Manuscripts are published online shortly after acceptance, before technical editing, formatting and proof reading. Using this free service, authors can make their results available to the community, in citable form, before we publish the edited article. We will replace this *Accepted Manuscript* with the edited and formatted *Advance Article* as soon as it is available.

You can find more information about *Accepted Manuscripts* in the [Information for Authors](#).

Please note that technical editing may introduce minor changes to the text and/or graphics, which may alter content. The journal's standard [Terms & Conditions](#) and the [Ethical guidelines](#) still apply. In no event shall the Royal Society of Chemistry be held responsible for any errors or omissions in this *Accepted Manuscript* or any consequences arising from the use of any information it contains.



Journal Name

ARTICLE

Experimental and Theoretical Photoluminescence Studies in Nucleic Acid Assembled Gold-Upconverting Nanoparticle Clusters

Liangcan He[‡],¹ Chenchen Mao[‡],² Suehyun Cho,² Ke Ma,¹ Weixian Xi,¹ Christopher N. Bowman,^{1,3} Wounjhang Park,^{2,3} * Jennifer N. Cha^{1,3} *

Received 00th January 20xx,
Accepted 00th January 20xx

DOI: 10.1039/x0xx00000x

www.rsc.org/

Combinations of rare earth doped upconverting nanoparticles (UCNPs) and gold nanostructures are sought as nanoscale theranostics due to their ability to convert near infrared (NIR) photons into visible light and heat, respectively. However, because the large NIR absorption cross-section of the gold coupled with their thermo-optical properties can significantly hamper the photoluminescence of UCNPs, methods to optimize the ratio of gold nanostructures to UCNPs must be developed and studied. We demonstrate here nucleic acid assembly methods to conjugate spherical gold nanoparticles (AuNPs) and gold nanostars (AuNSs) to silica-coated UCNPs and probe the effect on photoluminescence. These studies showed that while UCNP fluorescence enhancement was observed from the AuNPs conjugated UCNPs, AuNSs tended to quench fluorescence. However, conjugating lower ratios of AuNSs to UCNPs led to reduced quenching. Simulation studies both confirmed the experimental results and demonstrated that the orientation and distance of the UCNP with respect to the core and arms of the gold nanostructures played a significant role in PL. In addition, the AuNS-UCNP assemblies were able to cause rapid gains in temperature of the surrounding medium enabling their potential use as a photoimaging-photodynamic-photothermal agent.

Introduction

Due to the ability of rare earth doped upconverting nanoparticles (UCNPs) to absorb near infrared (NIR) radiation and emit visible light, there is considerable interest in their use for solar energy conversion,¹⁻³ biological imaging, and therapeutics.⁴⁻⁷ Compared with other traditional fluorescent materials such as quantum dots and organic dyes, UCNPs exhibit little background auto-fluorescence, high photostability, low toxicity, and tunable emission.^{4,8,9} More importantly, NIR has a penetration depth of up to several centimeters through typical biological tissues.¹⁰⁻¹² In addition to the imaging capabilities UCNPs have been combined with photosensitizers to generate singlet oxygen to induce cell toxicity via photodynamic therapy.^{7,13-15} Since metal nanostructures have been utilized for photothermal therapy via NIR excitation,¹⁶⁻¹⁹ combining UCNPs with metal nanocrystals would enable the delivery of a theranostic agent that could detect diseased sites *in vivo* while inducing both photodynamic and photothermal therapy at those locations. For this, to date most of the previous studies have focused on integrating Au or Ag nanostructures with UCNPs,²⁰⁻²³ including

Ag nanowires²⁴ or Au nanorods.²⁵ Because light absorption by these anisotropic structures depends strongly on the incident angle and polarization of the excitation light,^{22,26-28} their efficacy may be significantly reduced *in vivo*. While gold nanoshells that show tunable plasmon resonances have also been successfully coated onto UCNPs,^{27,29-31} the presence of a gold coating may limit or prevent the flow of analytes to and from the UCNPs or silica coated UCNPs, limiting their use as a photodynamic therapy agent.

We demonstrate here methods to couple spherical shaped Au nanostructures, specifically gold nanoparticles (AuNPs) and gold nanostars (AuNSs), to silica-coated NaYF₄:Yb/Er UCNPs through nucleic acid interactions.^{32,33} For this, we chose AuNPs and AuNSs whose plasmon resonances ranged from the visible to NIR region. For the photoluminescence (PL) measurements, the Au-UCNP clusters were dispersed in solution rather than drying on a substrate to better mimic the biological environment. The number and type of Au nanostructure were found to play a significant role in modulating the optical output from the UCNPs. The measurements showed that there is a distinct plasmon-dependent fluorescence that can be ascribed to the competition between the plasmon enhancement of the upconversion process and the extinction properties of the metal nanostructures. Furthermore, since the NIR dependent thermo-optical responses were observed only from the NIR absorbing AuNSs, it was critical to control and optimize the ratio of AuNSs to the UCNPs to allow usage as

¹Department of Chemical and Biological Engineering, ²Department of Electrical, Computer and Energy Engineering, ³Materials Science and Engineering, University of Colorado, Boulder

Email: won.park@colorado.edu, jennifer.cha@colorado.edu

‡These authors contributed equally to this work.

agents for imaging and photodynamic and photothermal therapy.

Experimental Section

Reagents and materials

L-ascorbic acid (98%), silver nitrate (99%), gold(III) chloride trihydrate (99.9+%), TritonX-100, Yttrium(III) chloride (99.99%), Ytterbium(III) chloride (99.99%), Erbium(III) chloride (99.9%), oleic acid (90%), ammonium fluoride (99.99%), tetraethylorthosilicate (99%), 3-aminopropyltriethoxysilane (99%), bis p sulfonatophenyl phenylphosphine dihydrate dipotassium salt (97%), cyclohexane (99.5%), Igepal CO-520 and ammonium hydroxide solution (30-33%) were all bought from Sigma Aldrich. 5 nm and 10 nm gold colloid were bought from TED Pella. Sodium Borohydride, sodium hydroxide (98.8%), dimethyl sulfoxide (99.7%), tris (2-carboxyethyl) phosphine hydrochloride and succinimidyl 4-(N-maleimidomethyl) cyclohexane-1-carboxylate (SMCC) were bought from Thermo Scientific. 1-octadecene (90%) was bought from Acros. DNA (thiol-A10) was bought from Integrated DNA Technologies, Inc. All the chemicals were used as received without further purification. Deionized water was used throughout the experiments.

Synthesis of NaYF₄:Yb, Er upconverting nanoparticles (UCNPs)

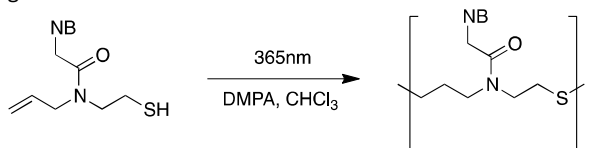
Monodisperse NaYF₄: 18%Yb, 2%Er UCNPs were synthesized using a previously reported method.³⁴ In a typical procedure, 0.1562 g YCl₃, 0.0503 g YbCl₃, and 0.0055 g ErCl₃ were mixed with 6 mL oleic acid and 15 mL octadecene. The solution was slowly heated to 160 °C with vigorous stirring under argon for 50 min to form a homogeneous transparent solution, and then allowed to cool to room temperature. Then, a 10 mL methanol solution of NaOH (0.1 g) and NH₄F (0.148 g) was added drop-by-drop and stirred for another 40 min. The solution was then slowly heated and degassed at 110 °C for 20 min, then refilled with argon and degassed three times total. After that, the solution was heated to 300 °C within 10 min and reacted for 1 h under argon. After the solution was cooled back to room temperature, the products were precipitated from the solution with ethanol and washed with ethanol and water (1:1) three times.

Synthesis of silica coated UCNPs

1.24 mg UCNPs were dispersed in 130 μL cyclohexane and sonicated for 30 min to give optically clear solutions. Then, ~3 μL Igepal CO-520 and 195 μL cyclohexane were added to this solution and stirred for 10 min. Next, ~13 μL Igepal CO-520 and 2.6 μL 30wt% ammonia were added and the container was sealed and sonicated for another 20 min. After that, 3.0 μL TEOS was added into the solution and the solution was shaken for 48 h. UCNPs@SiO₂ nanoparticles were precipitated by adding acetone, and washed with ethanol/water (1:1) three times. TEM analysis showed the thickness of the silica shell to be ~10nm.

Synthesis of polythymine clickable nucleic acid (CNA) strands³⁵

The deprotected monomer (1mmol) and 2,2-dimethoxy-2-phenylacetophenone (DMPA) 4 mg were dissolved in 0.8 mL CDCl₃. The solution was then irradiated by UV light (365 nm) for 30 min. The solution was removed to assess the conversion using ¹H-NMR. After the reaction time, a white precipitate was formed. The liquid fraction was decanted, and the precipitate was then rinsed with diethyl ether (4 × 3 mL) and methanol (4 × 3 mL). Filtration and drying yielded a white solid, which was subjected to MALDI-TOF and GPC analyses after drying under high vacuum.



Synthesis of CNA modified silica coated UCNPs

Briefly, 1.24 mg silica coated UCNPs were first reacted with 3-aminopropyltriethoxysilane (APTES) in ethanol (V_{APTES}:V_{ethanol}=5:95) for 5 h. Then the amine modified UCNPs@SiO₂ (in 10 μL H₂O) was reacted with 1.24 mg succinimidyl 4-(N-maleimidomethyl) cyclohexane-1-carboxylate (SMCC) (1.24 mg SMCC in 50 μL DMSO) for 5 h. The mixture was centrifuged and washed, then resuspended in 10 μL DMSO. 14 μL of polyT CNA solution (1 mg in 200 μL DMSO) was mixed with 5 μL tris(2-carboxyethyl)phosphine (TCEP) (50 mM in 200 mM NaHCO₃), then added to the SMCC modified UCNPs@SiO₂. The reaction was allowed to proceed overnight. Finally, the above products were purified and dispersed in DMSO solution for further use.

Preparation of DNA modified 520nm AuNPs, 700nm AuNSs and 980nm AuNSs

DNA-AuNPs

The citrate on the surface of AuNPs was first replaced by bis p sulfonatophenyl phenylphosphine dihydrate dipotassium salt (BSPP).³² Typically, 4.5 mg BSPP was added into 7 mL of the AuNPs solution and stirred overnight. Then, ~3 M NaCl was added slowly to the above solution until the color turned brown/blue. The as-prepared BSPP-AuNPs were purified by 30K Nanosep centrifuge filter for three times. For DNA attachment to AuNPs, freshly TCEP treated thiol-A10 and BSPP-AuNPs (DNA: BSPP-AuNPs=200:1) were mixed in 0.01 M NaCl solution and reacted overnight. The as-prepared materials were centrifuged and washed with water three times. Finally, the as-obtained DNA-AuNPs were dispersed in water solution and kept at 4 °C.

DNA-700nm AuNSs

In a typical procedure, 700nm AuNSs were prepared by a seed-mediated method.³⁶ 10 nm citrate stabilized commercial AuNPs were used as the seed (A₅₂₀=0.793). For 700 AuNSs synthesis, 300 μL of the commercial AuNPs were added into

9.5 mL 0.25 mM HAuCl₄ solution (with 100 μ L 0.1 M HCl) in a 20 mL vial at room temperature with moderate stirring. Then, 100 μ L 4 mM AgNO₃ and 50 μ L 100 mM ascorbic acid were simultaneously added into the above solution quickly. Immediately, the solution color turned blue, which indicated that AuNSs were obtained. The AuNSs solution was purified by centrifugation and redispersed in water. Then TCEP-treated thiol-A10 DNA (A10:AuNSs=1000:1) was added into the AuNS solution (in 0.01 M NaCl). The reaction was allowed to proceed for a few hours. In order to remove excess DNA, the solutions were centrifuged several times until the supernatants showed no more absorption at 260nm corresponding to the DNA strands.

DNA-980nm AuNSs

In a typical procedure, there are two steps for the synthesis.³⁷ Glassware used for the preparation were all pretreated before use by aqua regia for 30 min. First, the seed solution was prepared in a 20 mL glass vial. 0.5 mL 5×10^{-4} M HAuCl₄ and 0.5 mL 0.2 M TritonX-100 were added into the vial, then 0.06 mL ice-cold 0.01 M NaBH₄ aqueous solution was added. The seed solution was kept in ice and used within a few hours.

Second, the growth solution was prepared in another 20 mL vial. 250 μ L 4 mM AgNO₃, 5 mL 1 mM HAuCl₄, 5 mL 0.3 M TritonX-100 and 390 μ L 0.0788 M ascorbic acid were added into the vial. Immediately, the solution color turned to colorless. Quickly, 12 μ L of the aforementioned Au seed solution was added into the growth solution. After stirring for 1 h, the AuNSs was purified by centrifugation. The AuNSs solution was purified by centrifugation and was redispersed in water. Then TCEP treated thiol-A10 DNA (A10:AuNSs=1000:1) was added into the AuNSs solution (in 0.01 M NaCl). The reaction was allowed to proceed for a few hours. In order to remove excess DNA, the solutions were centrifuged several times until the supernatants showed no more absorption at 260nm corresponding to the DNA strands.

Preparation of Au-UCNP clusters

To prepare Au-UCNP clusters (for example, molar ratio of Au:UCNP=1:1), 10 μ L UCNP@SiO₂-CNA (48 nM) was mixed with 10 μ L DNA-Au (48 nM) and 80 μ L water to keep the total volume at 100 μ L. The mixture was rotated for at least 5 hours. A series of Au-UCNP clusters with a target Au:UCNP ratio was prepared by a similar procedure except for changing the added amount of DNA-Au solution.

Result and Discussion

The components of the assemblies reported in this work were chosen based on their reported or expected photophysical properties. Yb³⁺ and Er³⁺ doped upconverting nanoparticles (NaYF₄:Yb/Er UCNP) were first synthesized using a slightly modified procedure from Zhang *et al.*³⁴ From TEM analysis, the particles possessed an average diameter of \sim 20nm, and X-ray diffraction analysis showed the nanocrystals to have a

hexagonal structure (Figure 1 and Figure S1).³⁸ In order to transfer the as-synthesized surfactant capped UCNP to water

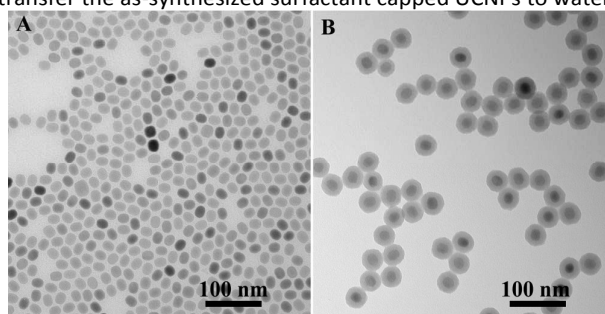


Fig 1. Transmission electron microscopy (TEM) images of as-prepared NaYF₄:Yb/Er (A) UCNP and (B) silica coated UCNP.

a microemulsion method was used to coat the surface of the as-synthesized UCNP with silica.³⁴ For this, the UCNP were first dispersed in cyclohexane followed by the addition of the surfactant Igepal and ammonia and reacted for 48 hrs to generate silica shells \sim 10nm in thickness (Figure 1).³⁴ The silica coatings were used to adjust the distance between the NaYF₄:Yb/Er NPs and the Au nanocrystals since previous work has shown that metal structures directly at the surface of the UCNP cause quenching.^{20,26} Next, gold AuNSs with plasmon resonances at \sim 700nm and \sim 980nm were synthesized using previously reported seeding methods (Figure 2).^{36,37} The AuNSs that showed a \sim 700nm plasmon possessed a uniform core size of \sim 26.1 nm with numerous branches, while

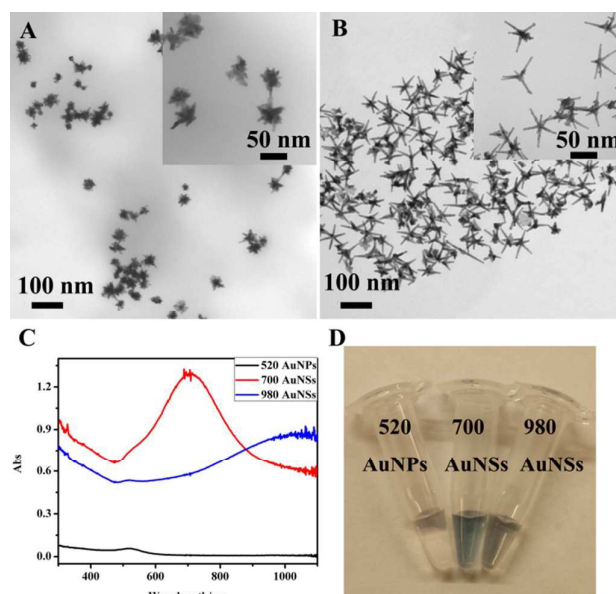


Fig 2. TEM images of the (A) AuNSs with plasmon at 700nm (700 AuNSs), (B) AuNSs with plasmon at 980nm (980 AuNSs), (C) UV-vis spectra of same concentration of 520 AuNPs, 700 AuNSs and 980 AuNSs, and (D) corresponding optical images.

the AuNSs with a 980nm plasmon had a core size of ~ 19.9 nm with 4 \sim 7 sharp tips per star (Figure 2 and Figure S2). Finally, 5nm AuNPs were obtained from a commercially available source (Ted Pella, Figure S3). At the same concentration of AuNSs and AuNPs, the AuNSs overall exhibited much greater absorbance than the AuNPs (Figure 2C, Figure S3-S5 and Table S1) which can be attributed to the much larger size of the AuNSs and is in accordance with Mie theory which predicts that the absorption cross-section increases linearly with the physical size of the metal nanostructure.³⁹

Next, nucleic acid interactions were utilized to couple the AuNPs and AuNSs with the silica coated UCNP. For this, both DNA and clickable nucleic acids (CNA) were tried due to the scalability of the CNA synthesis and potential backbone tunability as opposed to DNA.³⁵ After DNA conjugation to the Au nanocrystals and centrifugation or filtration, UV-Vis measurements of the corresponding eluents or supernatants, showed that ~ 76 and ~ 60 DNA strands were conjugated to the AuNPs and AuNSs respectively. The DNA conjugated Au nanostructures were next hybridized to the nucleic acid coated UCNP using molar ratios of Au:UCNP of 10:1, 5:1, 1:1, 0.5:1, 0.2:1, 0.1:1 and 0.05:1. To determine the concentration of the nucleic acid conjugated UCNP in the stock solution, a standard curve of UCNP photoluminescence (PL) intensity was first determined by weighing out the as-synthesized oleic acid coated UCNP and using both the particle volume as measured by TEM and a density of 4.727 g/cm³ (Figure S6) to determine UCNP concentration.⁴² This standard curve was then applied throughout to determine the concentration of silica coated UCNP and nucleic acid conjugated UCNP in solution. The concentrations of the DNA conjugated AuNSs in solution were determined using the extinction coefficients of the spherical gold cores in the centers of each star; the core mainly contributes to the 520nm peak while the branches determine the plasmon position and intensity in the NIR region (Figure S4 and S5).³⁶ After hybridizing the AuNPs and AuNSs to the UCNP, TEM analysis showed that the AuNPs and AuNSs were well conjugated to the UCNP (Figure 3, Figure S7). In the case of AuNSs, most of the interactions with the UCNP occurred at the tips of the branches and with all three types of Au, very few unbound Au was observed to be in solution. Furthermore, the solutions of the Au-UCNP showed no bulk aggregation and were optically clear (Figure 3). The overall colors of the

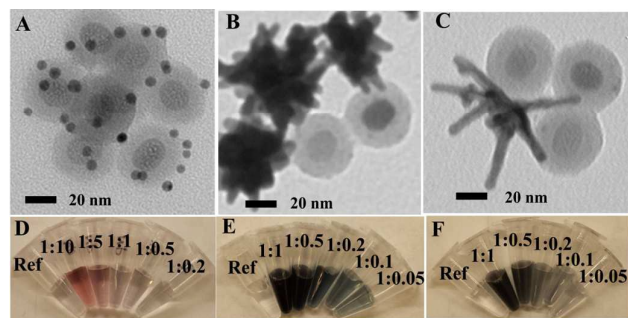


Fig 3. TEM images of the Au-UCNP clusters (A) AuNP-UCNP, (B) 700 AuNS-UCNP, (C) 980 AuNS-UCNP and (D-F) the

corresponding optical images. The molar ratios of AuNP:UCNP and AuNS:UCNP used here were 5:1 and 1:1 respectively.

solutions primarily depended on the type of Au nanocrystals and their concentrations. The three types of Au nanostructures were chosen for this study because of their varying plasmon resonances (520nm, 700nm, 980nm) which also overlapped with either the emission or excitation bands of the UCNP (Figure S8). In order to determine the effect of coupling the AuNPs and AuNSs to the UCNP (with ~ 10 nm silica shell), PL measurements were run of the Au-UCNP clusters dispersed in solution. While most UCNP PL measurements are run in the dry state, for biological applications and in particular photothermal therapy, the PL from ensembles of randomly configured nanoclusters dispersed in solvents needs to be probed. Samples were irradiated with a 980nm CW diode laser focused to produce an average power density of 69 kW/cm². The as made silica coated UCNP particles showed two emission bands centered at 545 nm and 660 nm, which correspond to

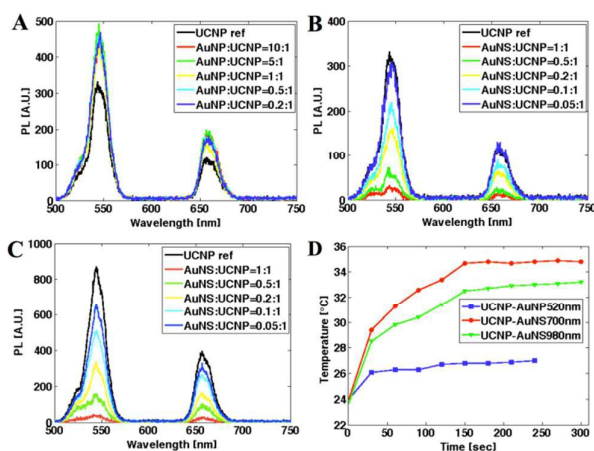


Fig 4. Fluorescence spectra of Au-UCNP clusters with different Au:UCNP ratios. (A) AuNP-UCNP (B) 700 AuNS-UCNP, (C) 980 AuNS-UCNP and (D) photothermal effect of these Au-UCNP clusters. The plot of temperature versus time was recorded upon irradiation by a 980nm laser (69 kW/cm²).

the $^2H_{11/2}/^4S_{3/2}$ to $^4I_{15/2}$ and $^4F_{9/2}$ to $^4I_{15/2}$ transitions respectively.^{21,43} Conjugation of the AuNPs and AuNSs caused significant changes to the UCNP fluorescence intensities that were strongly dependent on the number and type of Au added to the UCNP solution. For the AuNP-UCNP samples, molar AuNP:UCNP ratios of 0.2:1 to 10:1 showed an increase in PL in both the red and green emission peaks (Figure 4A). At AuNP:UCNP molar ratios higher than 10:1, however, a marked decrease in PL was observed (Figure S9).⁴⁴ The effect of Au loading per UCNP was drastically more pronounced with the AuNSs, where AuNS:UCNP ratios greater than 0.2:1 led to an overall decrease in fluorescence (Figure 4B and 4C). Only when the AuNS:UCNP molar ratio was less than 0.1 was no appreciable change in PL observed. Decreasing the AuNS:UCNP

ratio further to 0.05 did not lead to any gain in PL over UCNP alone for either type of AuNSs (plasmon at 700 and 980nm) (Figure S10). The strong dependence on the molar ratio and the overall decrease in fluorescence upconversion from AuNS-UCNP clusters are attributed to the highly complex local field profiles in the vicinity of the AuNS surfaces.

To substantiate the experimental observations, we conducted numerical simulations using the commercial software COMSOL (Figure S11-S13). The simulation details are given in the supplementary information. Briefly, a model for each type of Au nanostructure was constructed in accordance with the TEM and absorbance measurements. We then performed two types of simulations. First, the local field enhancement was investigated under the excitation of plane wave at various incidence angles and polarizations. The absorption enhancement was then obtained by the local intensity enhancement, $|E/E_0|^2$, where E and E_0 are the local electric field with and without the Au nanostructure. The emission enhancement was simulated by calculating the total emission from point dipoles at various locations. The total upconversion enhancement is then given by the product of absorption and emission enhancements (Table S2-S4). Since the samples largely consisted of an ensemble of randomly configured clusters of Au nanostructures and UCNPs, the overall enhancement of upconverted luminescence should be an ensemble average of all possible configurations which is not possible to faithfully simulate. Nevertheless, the numerical simulations do provide a key insight to the experimentally observed PL from Au-UCNP clusters. As shown in Figure 5, the local field profiles of AuNSs are highly non-uniform with distinct regions of strong field enhancement and quenching. The AuNPs exhibited local field intensity variations of only a few percent while AuNSs showed much greater variations, 0.60 to 2.00 for 700nm AuNSs and 0.96 to 1.59 for 980nm AuNSs. Similarly, the emission enhancement also showed wider fluctuations for AuNSs than for AuNPs. While the AuNSs show very large enhancement at some positions, they also have a larger volume of region exhibiting quenching. Thus, the ensemble average tends to show net quenching rather than enhancement. The full details of the simulation study are provided in the Supplementary Information. Our experimental observations backed by the simulations show what is realistically achievable in the eventual *in vivo* applications.

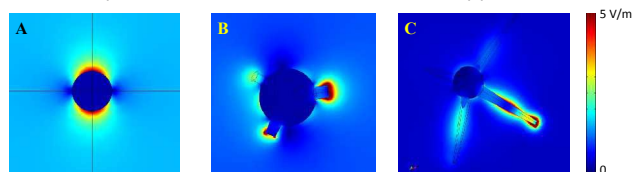


Fig 5. Electric field amplitude in the vicinity of (a) AuNPs, (b) AuNSs with 700 nm plasmon resonance and (c) AuNSs with 980nm plasmon resonance.

Next, the photothermal properties of the 0.2:1 AuNP-UCNP and 0.1:1 AuNS-UCNP clusters were studied. Since at these molar ratios of Au to UCNP, either an increase or little change in PL was observed as compared to the starting UCNPs, these self-assembled clusters could be potentially used for both imaging and photothermal therapy. For this, solutions of the AuNP-UCNP and AuNS-UCNP clusters were irradiated at 290 mW for 5 min while monitoring temperature via a thermocouple. After 150 s, almost no change in temperature was seen from the AuNP-UCNP clusters, but a dramatic 10 °C to 12 °C increase in temperature was observed for both types of AuNSs tested (Figure 4D). Since the AuNSs concentrations during these measurements were only 0.48 nM, by locally concentrating the AuNS-UCNP conjugates in the body, larger temperature increases can be gained upon exposure to NIR light. Furthermore, application of these constructs in the body whose basal temperature is 37 °C could potentially increase local temperatures to reach ~47-49 °C which is sufficient for cell apoptosis and possibly necrosis.⁴⁵ The elevated temperatures can also be confirmed by the ratios of the 524 and 545nm, which originate from the $^4H_{11/2} \rightarrow ^4I_{15/2}$ and $^4S_{3/2} \rightarrow ^4I_{15/2}$ transitions, respectively. Due to the close proximity of the two emitting levels, $^4H_{11/2}$ and $^4S_{3/2}$, their populations follow the simple Boltzmann distribution, resulting in $I(^4H_{11/2})/I(^4S_{3/2}) \propto \exp(-\Delta E/k_B T)$ where ΔE is the energy difference between the two levels, k_B is the Boltzmann constant and T is the temperature. Plotting the PL ratio against the temperature (Figure S14) allows us to determine ΔE . The fit yielded $\Delta E = 0.15 \pm 0.03$ eV, which was a little higher than the spectroscopically observed peak separation of 0.09 eV. The error is most likely due to the difficulty with measuring temperature of extremely small volume of solution. The PL results together with the thermo-optical response studies demonstrate that substantial heating is achievable without completely quenching the upconverted luminescence and that, in order to successfully synthesize a combined imaging, photodynamic therapy, and photothermal therapy agent, the concentrations and types of metal nanostructures must be carefully optimized relative to the amount of UCNPs.

Conclusion

In summary, novel NIR multifunctional Au-UCNP nanoclusters were constructed through nucleic acid mediated assembly. By carefully controlling the type and concentration of gold conjugated to the silica coated UCNPs, a theranostic agent that can potentially perform imaging, photodynamic and photothermal therapy was engineered. Gold nanostructures that show three-dimensional isotropy were chosen due to their tunable plasmon resonances that can reach the NIR region as well as their ability to respond independently of light polarization. These studies show that while NIR-responsive metal nanostructures such as AuNSs can generate rapid increases in temperature upon NIR excitation, their highly complex local field profiles can also cause significant photoluminescence quenching in UCNPs. While it may be feasible to use NIR responsive metal nanostructures that have

no overlapping resonances with either the excitation or emissive properties of UCNPs, the broad plasmon of synthesized metal nanocrystals makes this difficult to achieve experimentally. Thus this study shows that the optimal design of metal-UCNP constructs for combined imaging, photodynamic and photothermal therapy should adhere to using a single gold nanostructure bound with multiple UCNPs.

Acknowledgements

The research was supported in part by the U.S. Dept. of Energy (DOE), Office of Science, Basic Energy Sciences (BES) under Award # DE-SC0006398 (nanoparticle synthesis). L. He was also supported in part by DOE DE-SC0006398. In addition, the research was supported in part by the Office of Naval Research under Award # N00014-09-01-0258 and the Army Research Office under Award # W911NF-14-1-0211. We also acknowledge support from the National Science Foundation Award # DMR 1420736.

Notes and references

- W. Zou, C. Visser, J. A. Maduro, M. S. Pshenichnikov and J. C. Hummelen, *Nat. Photonics.*, 2012, **6**, 560-564.
- X. Huang, S. Han, W. Huang and X. Liu, *Chem. Soc. Rev.*, 2013, **42**, 173-201.
- J. C. Goldschmidt and S. Fischer, *Adv Opt Mater*, 2015, **3**, 510-535.
- J. Zhou, Q. Liu, W. Feng, Y. Sun and F. Li, *Chem. Rev.*, 2015, **115**, 395-465.
- Q. Liu, Y. Sun, T. Yang, W. Feng, C. Li and F. Li, *J. Am. Chem. Soc.*, 2011, **133**, 17122-17125.
- B. Dong, S. Xu, J. Sun, S. Bi, D. Li, X. Bai, Y. Wang, L. Wang and H. Song, *J. Mater. Chem.*, 2011, **21**, 6193-6200.
- N. M. Idris, M. K. Gnanasamandhan, J. Zhang, P. C. Ho, R. Mahendran and Y. Zhang, *Nat. Med.*, 2012, **18**, 1580-1585.
- J. Zhou, Z. Liu and F. Li, *Chem. Soc. Rev.*, 2012, **41**, 1323-1349.
- Y. I. Park, K. T. Lee, Y. D. Suh and T. Hyeon, *Chem. Soc. Rev.*, 2015, **44**, 1302-1317.
- L. R. Hirsch, R. J. Stafford, J. A. Bankson, S. R. Sershen, B. Rivera, R. E. Price, J. D. Hazle, N. J. Halas and J. L. West, *P. Natl. Acad. Sci.*, 2003, **100**, 13549-13554.
- R. Weissleder and V. Ntziachristos, *Nat. Med.*, 2003, **9**, 123-128.
- S. Stolik, J. A. Delgado, A. Pérez and L. Anasagasti, *Journal of Photochem. Photobiol B: Biol*, 2000, **57**, 90-93.
- Q. Q. Dou, A. Rengaramchandran, S. T. Selvan, R. Paulmurugan and Y. Zhang, *Sci. Rep.*, 2015, **5**, 8252
- S. S. Lucky, N. Muhammad Idris, Z. Li, K. Huang, K. C. Soo and Y. Zhang, *ACS Nano*, 2015, **9**, 191-205.
- C. Wang, H. Tao, L. Cheng and Z. Liu, *Biomaterials*, 2011, **32**, 6145-6154.
- M. S. Yavuz, Y. Cheng, J. Chen, C. M. Copley, Q. Zhang, M. Rycenga, J. Xie, C. Kim, K. H. Song, A. G. Schwartz, L. V. Wang and Y. Xia, *Nat Mater*, 2009, **8**, 935-939.
- Z. Zhang, J. Wang, X. Nie, T. Wen, Y. Ji, X. Wu, Y. Zhao and C. Chen, *J. Am. Chem. Soc.*, 2014, **136**, 7317-7326.
- H. Yuan, C. M. Wilson, J. Xia, S. L. Doyle, S. Li, A. M. Fales, Y. Liu, E. Ozaki, K. Mulfaul, G. Hanna, G. M. Palmer, L. V. Wang, G. A. Grant and T. Vo-Dinh, *Nanoscale*, 2014, **6**, 4078-4082.
- S. K. Cho, K. Emoto, L. J. Su, X. Yang, T. W. Flaig and W. Park, *J Biomed Nanotechnol*, 2014, **10**, 1267-1276.
- W. Park, D. Lu and S. Ahn, *Chem. Soc. Rev.*, 2015, **44**, 2940-2962.
- D. Lu, S. K. Cho, S. Ahn, L. Brun, C. J. Summers and W. Park, *ACS Nano*, 2014, **8**, 7780-7792.
- S. Han, R. Deng, X. Xie and X. Liu, *Angew. Chem. Int. Ed.*, 2014, **53**, 11702-11715.
- M. Saboktakin, X. Ye, S. J. Oh, S. H. Hong, A. T. Fafarman, U. K. Chettiar, N. Engheta, C. B. Murray and C. R. Kagan, *ACS Nano*, 2012, **6**, 8758-8766.
- W. Feng, L. D. Sun and C. H. Yan, *Chem. Commun.*, 2009, **29**, 4393-4395.
- N. J. Greybush, M. Saboktakin, X. Ye, C. Della Giovampaola, S. J. Oh, S. N. E. Berry, N. N. Engheta, C. B. Murray and C. R. Kagan, *ACS Nano*, 2014, **8**, 9482-9491.
- D. M. Wu, A. García-Etxarri, A. Salles and J. A. Dionne, *J. Phys. Chem. Lett.*, 2014, **5**, 4020-4031.
- H. Zhang, Y. Li, I. A. Ivanov, Y. Qu, Y. Huang and X. Duan, *Angew. Chem. Int. Ed.*, 2010, **49**, 2865-2868.
- A. L. Feng, M. L. You, L. Tian, S. Singamaneni, M. Liu, Z. Duan, T. J. Lu, F. Xu and M. Lin, *Sci. Rep.*, 2015, **5**, 7779.
- L. Sudheendra, V. Ortalan, S. Dey, N. D. Browning and I. M. Kennedy, *Chem. Mater.*, 2011, **23**, 2987-2993.
- L. Li, K. Green, H. Hallen and S. F. Lim, *Nanotechnology*, 2015, **26**, 025101.
- W. Deng, L. Sudheendra, J. Zhao, J. Fu, D. Jin, I. M. Kennedy and E. M. Goldys, *Nanotechnology*, 2011, **22**, 325604.
- H. Noh, A. M. Hung and J. N. Cha, *Small*, 2011, **7**, 3021-3025.
- H. Noh, C. Choi, A. M. Hung, S. Jin and J. N. Cha, *ACS Nano*, 2010, **4**, 5076-5080.
- Z. Li, Y. Zhang and S. Jiang, *Adv. Mater.*, 2008, **20**, 4765-4769.
- W. Xi, S. Pattanayak, C. Wang, B. Fairbanks, T. Gong, J. Wagner, C. L. Kloxin, C. N. Bowman, 2015, submitted
- H. Yuan, C. G. Khoury, H. Hwang, C. M. Wilson, G. A. Grant and T. Vo-Dinh, *Nanotechnology*, 2012, **23**, 075102.
- P. Pallavicini, A. Dona, A. Casu, G. Chirico, M. Collini, G. Dacarro, A. Falqui, C. Milanese, L. Sironi and A. Taglietti, *Chem. Commun.*, 2013, **49**, 6265-6267.
- F. Wang, Y. Han, C. S. Lim, Y. Lu, J. Wang, J. Xu, H. Chen, C. Zhang, M. Hong and X. Liu, *Nature*, 2010, **463**, 1061-1065.
- C. F. Bohren and D. R. Huffman, *Absorption and Scattering of Light by Small Particles*, Wiley-VCH Verlag GmbH & Co. KGaA, Weinheim, 2008.
- P. F. Xu, A. M. Hung, H. Noh and J. N. Cha, *Small*, 2013, **9**, 228-232.
- P. F. Xu, J. H. Lee, K. Ma, C. Choi, S. Jin, J. Wang and J. N. Cha, *Chem. Commun.*, 2013, **49**, 8994-8996.
- Z. Li, S. Lv, Y. Wang, S. Chen and Z. Liu, *J. Am. Chem. Soc.*, 2015, **137**, 3421-3427.
- S. Schietinger, T. Aichele, H.-Q. Wang, T. Nann and O. Benson, *Nano Lett*, 2010, **10**, 134-138.
- Y. Ding, X. Zhang, H. Gao, S. Xu, C. Wei and Y. Zhao, *J. Lumin.*, 2014, **147**, 72-76.
- P. Cherukuri, E. S. Glazer and S. A. Curley, *Adv. Drug Delivery Rev.*, 2010, **62**, 339-345.